Attenuation of lipopolysaccharide-induced lung inflammation by ascorbic acid in rats: Histopathological and ultrastructural study

Hazem Abdelhamid Mohamed[1,2], Yasser M Elbastawisy[1,3]
and Wael M Elsaed[1,3] (iD)

Abstract

Introduction: Lipopolysaccharide is a bacterial endotoxin that induces acute lung injury in experimental animals, which is similar to acute respiratory distress syndrome in humans. The induced tissue trauma ends in fibrosis. Understanding the pathogenesis is important in the prevention and treatment of the complications. This study was assigned to investigate the long-term lipopolysaccharide-induced lung injury and the postulated protective effect of ascorbic acid on these changes.

Materials and methods: Twenty-four adult male albino rats were divided into three groups. Group I was the controls, group II received lipopolysaccharide and group III received lipopolysaccharide and ascorbic acid. After 30 days of starting treatment, lung tissue samples were obtained.

Results: Group II lung tissues showed marked thickening of the alveolar septa with collapsed alveolar sacs, detached bronchial epithelium, inflammatory cell infiltration and excessive deposition of collagen. Group III showed mild thickening of the alveolar walls, scanty inflammatory cell infiltration, mild parabronchial fibrosis and less marked collagen deposition. α-Smooth muscle actin staining of group II showed marked expression of the actin-positive cells. Less potential expression of the dye was found in group III. Ultrastructural examination of group II showed evident structural changes in pneumocytes with capillary basement membrane irregularity and interruption compared to uniform basement membrane in group III with less prominent intracellular changes in pneumocytes.

Conclusion: Ascorbic acid attenuated the inflammatory response and fibrosis in the lungs of rats treated with lipopolysaccharide as evidenced by the histological, immunohistochemical and ultrastructural studies.

Keywords

Lung fibrosis, ascorbic acid, α-smooth muscle actin

Introduction

Lipopolysaccharide (LPS) is a bacterial endotoxin derived from the cell wall of the Gram-negative bacteria. It is a widely accepted experimental inducer of acute lung injury (ALI).[1,2] LPS-induced ALI in experimental animals simulates acute respiratory distress syndrome in humans.[3] It acts by activation of the immune system in a similar way to severe sepsis by causing systemic inflammation with production of reactive oxygen species (ROS), which initiates lung tissue injury by oxidative affection of the lung microvasculature.[4–6] This injury ends with severe hypoxemia[7–9] and inflammatory cell infiltration.[10,11] The cellular infiltration starts in the blood capillaries and then in the interstitial tissue accompanied by hypertrophy of interstitial fibroblasts.[6] By time, the induced tissue dysfunction and tissue trauma end in fibrosis.[6,12,13]

The body defends against ROS by antioxidant enzymes when the production of the free radicals exceeds the enzymatic system capacity, and the second line of defense (vitamins) may come into action.[14] Therapeutic measures that can control or neutralize the produced ROS are therefore able to

[1]Department of Anatomy and Embryology, Faculty of Medicine, Taibah University, Madinah, Saudi Arabia
[2]Department of Human Anatomy and Embryology, Faculty of Medicine, Assiut University, Assiut, Egypt
[3]Department of Anatomy and Embryology, Faculty of Medicine, Mansoura University, Mansoura, Egypt

Corresponding author:
Wael M Elsaed, Department of Anatomy and Embryology, Mansoura Faculty of Medicine, Dkahlia 35516, Mansoura, Egypt.
Email: wzaarina@yahoo.com

modulate inflammatory cell migration reversing ROS-mediated pulmonary injury. Previous studies on ROS scavengers on endotoxin-induced ALI proved significant reduction in parameters of tissue injury with an improvement in the pulmonary functions.[15]

Ascorbic acid is the commonest nontoxic essential dietary antioxidant.[16] It is the reduced form of vitamin C, which is an essential metabolite for life.[17] It has been proved to act against sepsis-induced inflammation.[18] It prevents oxidation of cytoplasmic and membrane components of cells[19] through scavenging reactive oxygen and nitrogen species[20] or by promoting the action of antioxidant enzymes.[21]

Plasma concentration of ascorbic acid was found to be subnormal in patients with sepsis or organ failure.[18,22] At the same time, its deficiency was always found to be associated with increased oxidative stress and oxidant-induced cell death.[23]

The implied mechanisms of short-term inflammatory process during LPS-induced ALI were discussed in previous researches;[24,25] however, facts about the long-term tissue changes are still deficient and need more investigations. Understanding these pathological changes is important for effective prevention and treatment.[26] This study was therefore assigned to investigate the long-term LPS-induced lung injury and the postulated protective effect of ascorbic acid on these changes.

Materials and methods

Animals and groups

Twenty-four adult male albino rats (200–240 g weight) of 12–14 weeks were obtained from Mansoura Faculty of Medicine animal house. The sample size was calculated by OpenEpi calculator. The variables reading entered according to similar previous studies.[2,5] They were kept in five rat cages under the standard conditions approved by the Institutional Research Board (IRB) of Mansoura University.

All animal handling procedures were conducted in accordance with the principles of laboratory animal care (National Institutes of Health Guide for the Care and Use of Laboratory Animals; NIH Publications No. 8023, revised 1978). After 7 days of acclimatization, rats were divided into three groups (eight animals each). Group (I) served as the controls, group (II) received LPS (*Escherichia coli* LPS, 055: B5, Product Number: L2880) purchased from Sigma Aldrich (St. Louis, MO, USA) in phosphate-buffered saline (PBS; Sigma Aldrich, Product Number: P7059) and group (III) received LPS and ascorbic acid (Vitamin C; Memphis Co. for Pharmaceutical and Chemical Industries, AstraZeneca, Egypt, product of Toronto Research chemicals, Product Number: A786990, supplied as white powder, dissolved in sterile distilled water and prepared as an aqueous solution). Group (II) animals were injected with LPS dissolved in 4 µL of PBS 10 mg/kg rat intraperitoneally. The injection was repeated after 5 days in a dose of 5 mg/kg to induce lung injury.[27] Group (I) animals received an equal

volume of PBS intraperitoneally at the same time. Group (III) received LPS (similar to group II) and ascorbic acid (250 mg/kg/day) for 30 days via gastric tube starting from the first day of LPS exposure.[28]

Experimental protocols

After 30 days of starting treatment, no mortality was detected. All rats were killed by exsanguination under anesthesia with 80 mg/kg ketamine (Ketamine, Pfizer, USA, Product Number: PL 01502/0099) and 5 mg/kg xylazine (xylazine hydrochloride Buyers Helpdesk, India, Product of Sigma Aldrich, Product Number X 1126). The thoracic cavities were opened in the midline; the lungs were exposed, detached and prepared for light and electron microscopic studies.

Light microscopic study

Lung tissue specimens (four specimens per rat) were stained by the usual techniques of H&E (Sigma Aldrich, Product Number: HHS16 and E4009), Masson's trichrome (MT) (Sigma Aldrich, Product Number: HT15) and Sirius Red stains (Sigma Aldrich, Product Number: 365548) for detection of tissue fibrosis[29] and anti-α-smooth muscle actin (Anti-Actin, smooth muscle Antibody, clone ASM-1/1A4, Product Number: A2547, Sigma Chemical Co., St. Louis, MO, USA) immune stain for detection of myofibroblast activity.[30]

Electron microscopic examination

Ultrathin sections (50–70 nm) were stained with uranyl acetate and lead citrate (Product of TED PELLA INC. USA, Product Number 155) and examined in Assiut electron microscope unit (Joel X100 CXII TEM at Assiut Electron Microscope Unit and photographed using Digital Camera CCD Jacan, Model XR).[31]

Image analysis

The area percent of collagen deposition in Masson's trichrome–stained sections of the similar lung areas was estimated by optical density in randomly selected alveolar septa using Leica Q Win standard (digital camera CH-9435 DFC 290, Germany). For all measures, 10 non-overlapping fields in each paraffin block for each rat were examined at ×400 magnification and photographed. The lamp intensity, camera exposure and camera gain were kept constant throughout the examination. The photographs were analyzed for positive staining using an Image Analyzer with a measuring frame area = 786,432.0 µm^2. Morphometry was carried out at the Image Analysis Unit, Anatomy Department, Faculty of Medicine, Taibah University.

Sirius red–stained sections (10 non-overlapping fields in each paraffin block for each rat) were examined randomly under ×100 power by two observers in a blind manner. Quantitative analysis was performed using a validated,
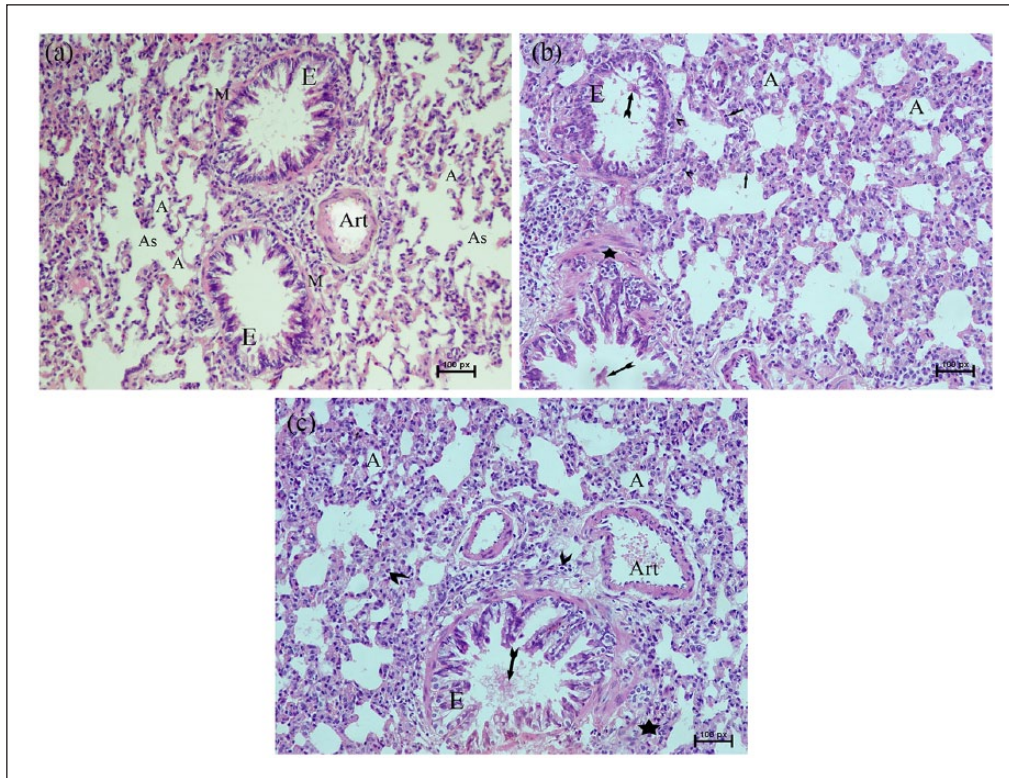
Figure 1. (a) Photomicrograph of control lung showing multiple alveoli (A) with numerous alveolar sacs (AS). Terminal bronchioles are seen lined with ciliated columnar epithelium (E) with a smooth uniform layer of smooth muscle (M). A pulmonary arteriole is seen close to the bronchioles. (b) Photomicrograph of group II lung tissue showing collapsed obliterated alveolar air spaces (A) with thickening of the interalveolar septa containing multiple apoptotic cells (arrow) and widespread inflammatory cell infiltration (arrowheads). The bronchiolar epithelium (E) shows areas of patchy separation with accumulated sloughed epithelial cells and amorphous material in the lumen (tailed arrows). Scattered nodules of linearly arranged spindle-shaped fibroblasts with pale staining extracellular matrix are also seen (star). (c) Photomicrograph of group III lung tissue showing mild thickening of the alveolar walls (A) with scanty inflammatory cell infiltration (arrowheads). Less congested arterioles (Art) with less apparent parabronchiolar fibrosis (star). Bronchiolar epithelium (E) appears intact with a small amount of amorphous material in the lumen (tailed arrow).

arbitrary visual scale with grading scores of 0, 1, 2, 3 and 4 representing no, weak, moderate, intense and very intense staining, respectively.[32,33] Data from both studies were expressed as mean ($\pm$ SD).

Statistical analysis

Data collected from the morphometric study of Masson's trichrome–stained sections of different groups were analyzed using ANOVA (analysis of variance) test. A two-tailed Mann–Whitney rank-sum test was used for non-parametric comparisons of the quantitative data obtained from Sirius red–stained sections. A *p*-value of $p < 0.001$ indicates significant differences.

Results

Light microscopic examination

Light microscopic examination of group I (control group) revealed normal lung tissue structure including multiple alveoli with alveolar sacs, terminal bronchioles lined with ciliated columnar epithelium and a layer of smooth muscle fibers and pulmonary arterioles with uniform thickened walls (Figure 1(a)).

Group II lung tissues showed marked histopathological changes in the form of thickened irregular alveolar septae with multiple apoptotic cells. Most alveolar sacs were collapsed with obliterated lumens. Areas of patchy detachment of the bronchiolar epithelium with sloughed epithelial cells show amorphous material in its lumens. Widespread areas of septal edema with interstitial inflammatory cell infiltration were also evident. Scattered nodules of linearly arranged spindle-shaped fibroblasts with pale staining extracellular matrix were also seen. Congested blood vessels with hypertrophy of the muscle layer were observed (Figure 1(b)).

In contrast, group III lung tissues showed mild thickening of the alveolar walls, scanty inflammatory cell infiltration, intact bronchiolar epithelium with scarce cellular debris and mild parabronchial fibrosis (Figure 1(c)).
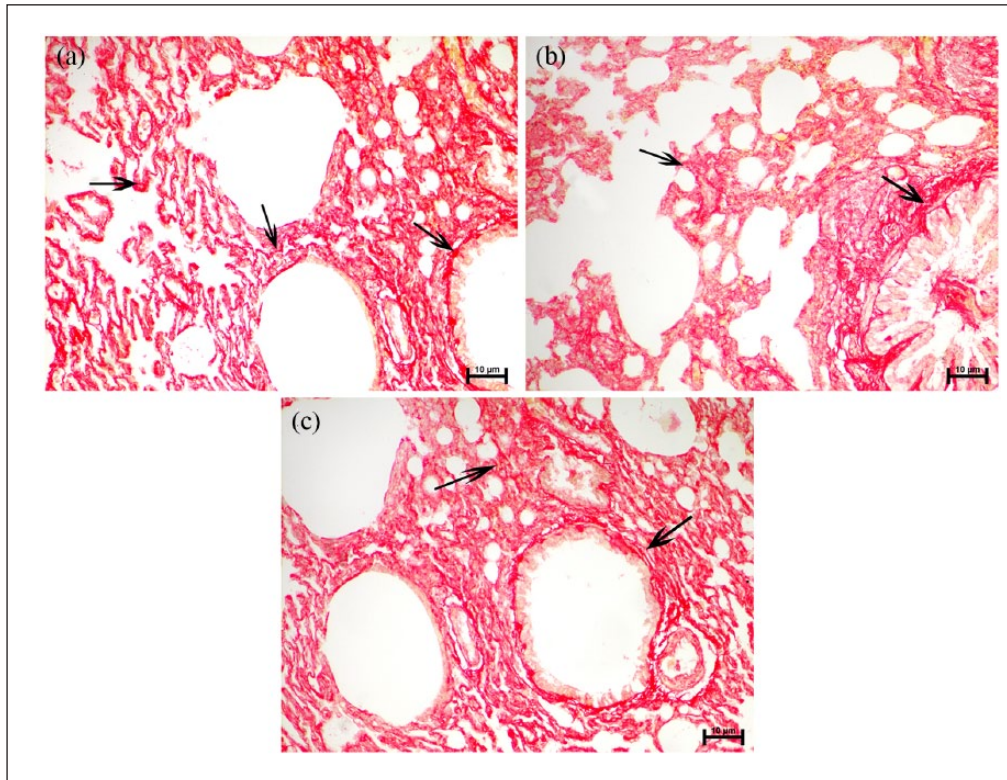
Figure 2. (a) Photomicrograph of control lung tissue stained with Sirius red stain shows normal pulmonary architecture with normal fibrous tissue distribution in both bronchiolar wall and pulmonary interstitium (arrows). (b) Photomicrograph of group II lung tissue stained with Sirius red stain shows excessive collagen deposition in both bronchiolar wall and pulmonary interstitium (arrows). (c) Photomicrograph of group III stained with Sirius red shows less marked bronchiolar and interstitial collagen bundles deposition (arrows).

Sirius red stain revealed minimal fibrous tissue distribution in both bronchiolar walls and pulmonary interstitium of the control group (Group I) (Figure 2(a)). Group II lung tissue showed excessive deposition of collagen especially in the perivascular spaces and subepithelial matrix (Figure 2(b)). Compared with group II, lung tissues of group III showed apparent less marked collagen deposition (Figure 2(c)).

Masson's trichrome stain of the control lung tissue showed minimal interstitial fibrosis (Figure 3(a)). Group II showed extensive collagen deposition in the bronchiolar walls and the pulmonary interstitium (Figure 3(b)), while group III showed less enhanced pulmonary fibrosis (Figure 3(c)).

α-Smooth muscle actin (SMA) staining of the control lung tissues (group I) showed minimal actin-positive cell expression particularly in the bronchiolar wall and adjacent blood vessels (Figure 4(a)). On the contrary, extensive expression of the actin-positive cells, particularly in the fibrotic foci, was seen in group II (Figure 4(b)). Less potential expression of the dye was found in the lung tissues of group III (Figure 4(c)).

Electron microscopic examination

Transmission electron microscopic examination of the lung tissue of group I (control group) (Figure 5(a1) and (a2)) showed apparently normal alveolar septae formed of type I pneumocytes with elongated nuclei and type II pneumocytes with a large rounded nuclei and numerous cytoplasmic organelles including lamellar inclusion bodies, rounded mitochondria, rough endoplasmic reticulum and numerous microvilli on the free border facing the alveolar space. The blood–air barrier is formed of peripheral cytoplasmic processes of the type I pneumocytes and the blood capillary endothelium with a common basement membrane in-between.

Group II lung tissues showed type II pneumocytes with shrunken dark eccentric nuclei, apical lamellar bodies, bizarre-shaped mitochondria and almost absent microvilli on the free border. The capillary basement membrane appeared irregular and interrupted. The interstitial space was widened with abundant collagen bundles and macrophage invasion (Figure 5(b1) and (b2)).

Electron microscopic examination of group III lung tissue (Figure 5(c1) and (c2)) revealed less prominent collagen bundle deposition and thick uniform basement membrane. Type II pneumocytes showed rounded mitochondria, few lamellar inclusion bodies and near-normal microvilli.

Morphometric analysis

Morphometric analysis of the area percent of collagen deposition of Masson's trichrome–stained sections showed a significant increase of collagen content in lung tissues of group II rats compared to the control group. Ascorbic
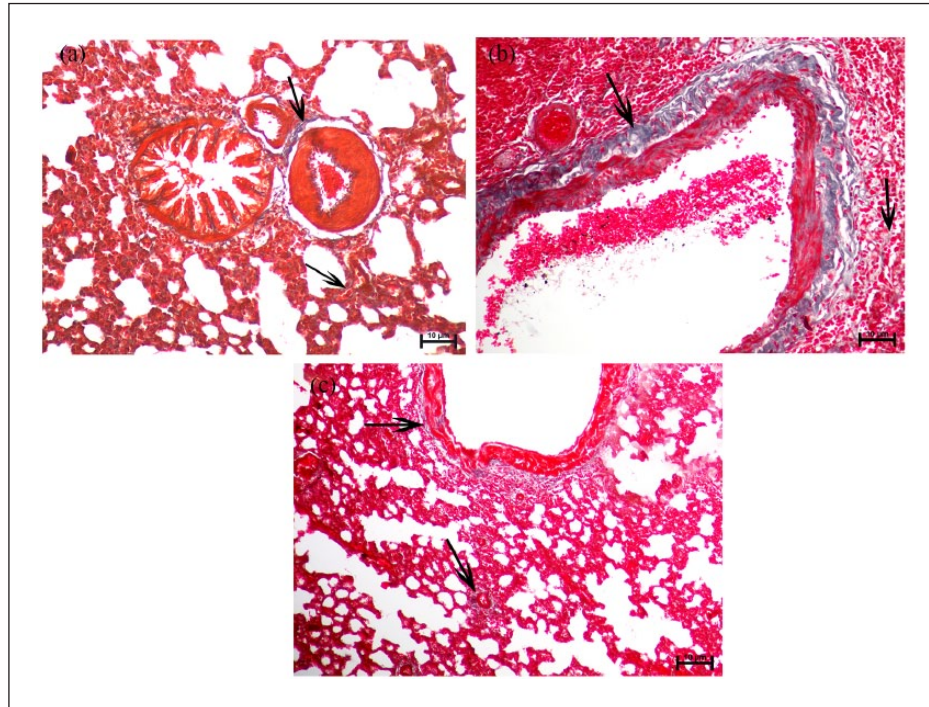
Figure 3. (a) Photomicrograph of control lung stained with Masson's trichrome stain shows a thin layer of collagen bundles in the bronchiolar wall with scanty bundles in the interstitium (arrows). (b) Photomicrograph of group II lung stained with Masson's trichrome stain shows excessive collagen deposition in the bronchial wall and interstitium (arrows). (c) Photomicrograph of group II lung stained with Masson's trichrome stain shows less enhanced pulmonary fibrosis both in the bronchial wall and the interstitium (arrows).
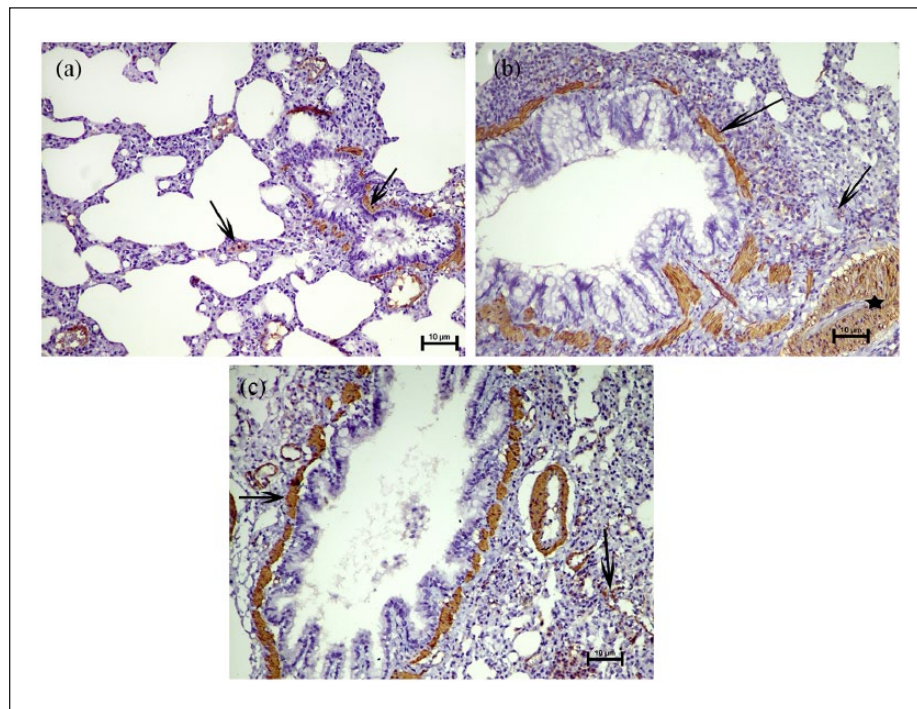

Figure 4. (a) Photomicrograph of control lung stained with α-smooth muscle actin shows minimal expression of actin-positive cells in the bronchiolar wall and the adjacent blood vessels (arrows). (b) Photomicrograph of group II lung stained with α-smooth muscle actin shows extensive expression of actin-positive cells in the bronchiolar wall (arrows). Aggregation of positive cells is identified in a fibrotic focus (star). (c) Photomicrograph of group III lung stained with α-smooth muscle actin shows less potential expression of the dye in the bronchiolar wall, the adjacent blood vessel and the interstitium (arrows).
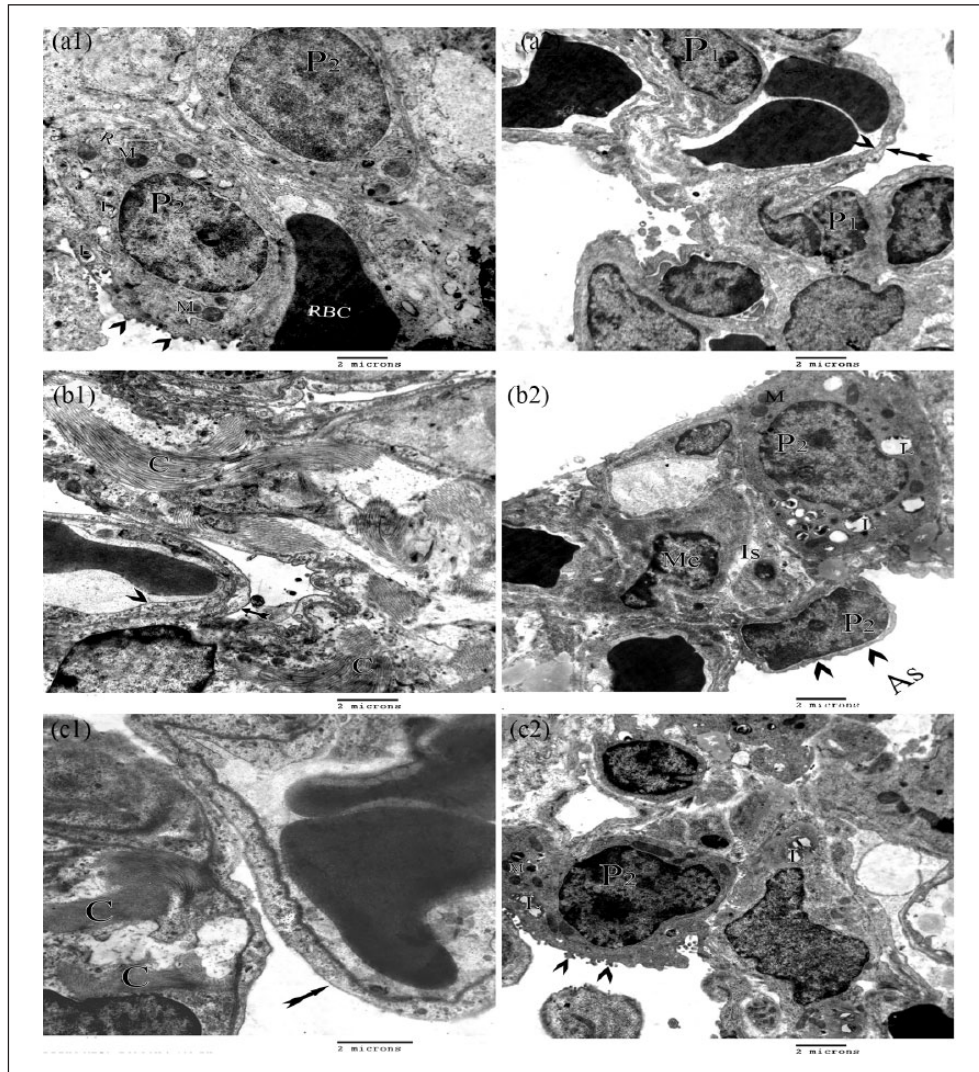
Figure 5. (a1) Electron micrograph of control lung shows type 2 pneumocyte (P2) with a large rounded nucleus, intracellular lamellar bodies (L), rounded mitochondria (M) and rough endoplasmic reticulum (R). The free border of the cell shows numerous microvilli (arrowheads) facing the alveolar space. A red blood cell (RBC) is seen in the pulmonary capillaries. (a2) Electron photomicrograph of control lung shows RBCs inside the pulmonary capillaries. Blood–air barrier formed of a peripheral cytoplasmic process (tailed arrow) of type 1 pneumocytes (P1) and the blood capillary endothelium (arrowhead) with a common basement membrane in-between. (b1) Electron micrograph of group II showing thickening of the irregular interrupted basement membrane in between endothelium (arrowhead) and the cytoplasmic process of P1 (tailed arrow). Numerous collagen bundles (C) are interposed in the interstitium. (b2) Electron photomicrograph of group II shows P2 cells with a shrunken dark eccentric nucleus, atypical lamellar bodies, bizarre-shaped mitochondria (M), intracellular lamellar bodies (L) and almost absent microvilli (arrowheads) toward the alveolar space (As). A microphage with an irregular nucleus (Mc) is seen in the expanded interstitium (Is). (c1) Electron photomicrograph of lung of group III shows less prominent collagen bundle deposition in the interstitium (C). The blood–air barrier (tailed arrow) shows thick and almost uniform basement membrane. (c2) Electron photomicrograph of group III shows P2 cells with mitochondria (M), intracellular lamellar bodies (L) and microvilli (arrowheads) toward the alveolar space.

acid–treated animals (group III) had a significant decreased collagen contents in lung tissues when compared to group II (Table 1 and Diagram 1).

Correlation between the scores of fibrosis in the lung tissues stained with Sirius Red stain (Table 2 and Diagram 2) showed that increased score of fibrosis in group II was significant compared to the control group and group III. A comparison of the scores between the individual readers showed no significant difference.

Discussion

LPS-induced lung injury is a widely accepted animal model of ALI.[25] LPS activates an inflammatory cascade in the endothelial cells resulting in stimulating collagen deposition in the extracellular matrix ending in tissue stiffening and fibrosis[1] which in turn exacerbates the inflammatory activation of lung vascular endothelium[34] and disruption of the endothelial barrier.[35]

Table 1. Morphometric measurements of the area of collagen deposition of lung tissue in square micrometers in Masson's trichrome–stained sections.

Control (Group I)	Group II	Group III
17.12 ± 0.69	34.9 ± 2.50*	25.6 ± 2.26*

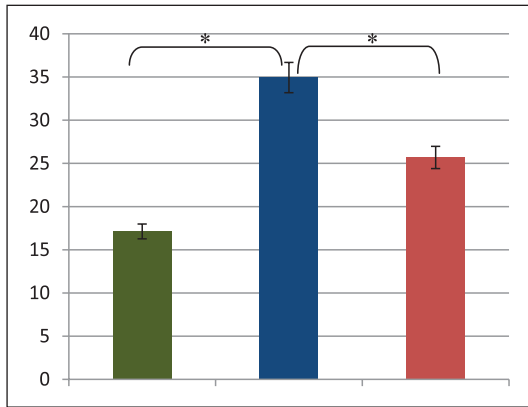Values are means ± SD.
*$p < 0.001$ significant.

Diagram 1. Area of collagen deposition of lung tissue in square micrometers.

Table 2. Scores of fibrosis in the lung tissues stained with Sirius Red stain.

Control (Group I)	Group II	Group III
1.03 ± 0.1	3.18 ± 0.16*	2.35 ± 0.257*

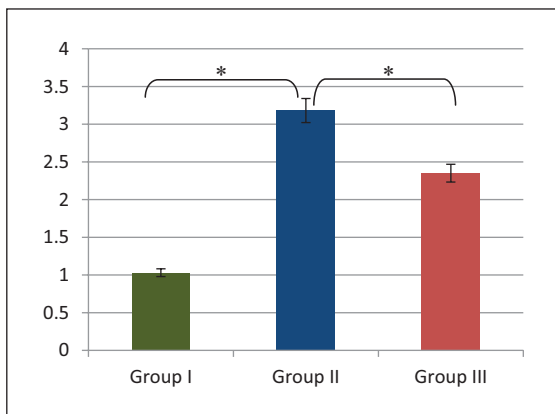Values are means ± SD.
*$p < 0.001$ significant.

Diagram 2. Score of fibrosis of lung tissue.

LPS-induced acute inflammation is completely established within a week. This process is followed by the development of chronic lung fibrosis[36] that is well settled around days 21–28.[26] In this study, the time of tissue sampling was at 30 days from the first LPS exposure to be sure that all the pathological changes are well established.

Our results showed that LPS-treated group (Group II) had thickened irregular alveolar septae with widespread areas of interstitial inflammatory cell infiltration and scattered nodules of fibroblasts. Same results were found in other studies[37,38] with more or less degrees of tissue inflammatory signs. This variability is mostly caused by the different LPS doses or timing of tissue sampling. On the other hand, ascorbic acid–treated group (Group III) lung tissues had less thickening of the alveolar walls, scanty inflammatory cell infiltration, intact bronchiolar epithelium and mild fibrosis.

Ultrastructural examination of the lungs of the group II showed cellular degeneration signs in type II pneumocytes with a widening of the interstitial spaces compared with the control group. Evident collagen deposition, microphage infiltration and irregularity of the capillary basement membrane indicate enhanced fibrosis. Similar results were discussed by Parra et al.[39] Less marked pathological changes were found in group III.

The extent of lung tissue fibrosis was estimated by collagen-specific dyes and confirmed by statistical analysis of collagen deposition. Group II showed excessive deposition of fibrous tissue in the perivascular spaces and subepithelial matrix. This deposition was statistically highly significant compared to the control group. Meanwhile, group III showed a significant decrease in collagen contents compared with group II.

Although being one of the major components in most body tissues,[40] collagen increased presentation is one of the main consequences of tissue inflammation. Different degrees of satisfaction of collagen fibers' staining methods have been reported.[41] Of the famous traditional histochemical methods, Masson's trichrome and Sirius red staining are outstanding. The degree of sensitivity of the dye is crucial in identifying the degree of tissue fibrosis. Some studies blamed Masson's trichrome stain to be the cause of underestimation of the collagen content.[42,43] Comparing the results of the two staining methods, the study is supposed to be more expressive and to avoid pitfalls of a single one. Results obtained from assessments of both dyes were almost similar.

LPS induces systemic inflammation with increased production of ROS, which initiates and promotes lipid peroxidation that ends in oxidative damage.[44] ROS are accused to be the main generator of lung fibrosis.[45,46]

Being one of the essential antioxidants, ascorbic acid can counteract the mechanism by which LPS induces lung inflammation and fibrosis. This is because it not only acts as a scavenger for ROS but also promotes the action of antioxidant enzymes.[21,47,48] Consequently, ascorbic acid reduces the high microvasculature permeability that characterizes acute lung inflammation following infusion of endotoxins like LPS.[5,37]

α-SMA staining of group II rats showed extensive expression of the actin-positive cells particularly in the fibrotic foci

compared with the control group. Less potential expression of the dye was observed in the lung tissues of group III.

α-SMA-positive cells are responsible for remodeling of fibrotic rat lungs.[49] The α-SMA-positive cells correspond to true alveolar myofibroblasts which proliferate and produce an accumulation of extracellular matrix in response to fibrotic stimuli. Slight changes in the total actin content of the lung are reflected by a considerable increase in α-SMA-positive cells.[30] The process of lung tissue fibrosis promotes proliferation and polymerization of actin content of fibroblasts.[30] During the process of fibrosis, the actin-containing cells accumulate and increase the extracellular matrix which results in increased contractility and decreased elasticity of the alveolar tissue.[50] On the biochemical level, LPS-induced inflammatory process is associated with increased fibronectin with subsequently increased tissue stiffening.[51] Ascorbic acid opposes this action as evidenced by the decreased expression of the dye in the lung tissues of group III. This action occurs mostly by inducing relaxation of the smooth muscles in the respiratory tree through increasing release of prostaglandin E2 and counteracting PGF2 alpha and histamine.[52]

Scavengers of ROS like ascorbic acid fortunately have the ability to reduce pulmonary hypertension, hypoxia and increased microvascular permeability, which characterize ALI following infusion of endotoxin.[5,37]

Poor management of lung inflammation may lead to the development of pulmonary fibrosis due to the resulting fibro-proliferative respiratory distress.[1] Pulmonary fibrosis is a major clinical problem with fatal outcome.[14] The disappointing and controversial results of traditional pharmacologic trials for management of pulmonary fibrosis create a necessity to look for effective protective management to treat or even to stop the progression of the disease.[48] At the same time, some of the proposed treatments were complicated with an increased risk of disease progression or severe side effects.[53]

The results of this study are limited by the relatively small number of animals and the high dosage of ascorbic acid used. Further investigations of the exact molecular mechanism involved in the protective effect of ascorbic acid on the lung tissue required to gain a better picture of its contribution to the lung repair.

Conclusion

Our study confirmed that ascorbic acid can attenuate the inflammatory response and fibrosis in the lungs of rats treated with LPS as evidenced by the histological, immunohistochemical and ultrastructural studies. These findings provide an evidence that ascorbic acid may serve as a target adjuvant therapy for potential protective treatment of post-inflammatory lung fibrosis.

Declaration of conflicting interests

The author(s) declared no potential conflicts of interest with respect to the research, authorship, and/or publication of this article.

ORCID iD

Wael M Elsaed https://orcid.org/0000-0001-7142-292X

References

1. Meng F, Mambetsariev I, Tian Y, et al. Attenuation of lipopolysaccharide-induced lung vascular stiffening by lipoxin reduces lung inflammation. *Am J Respir Cell Mol Biol* 2015; 52: 152–161.
2. Iraz M, Iraz M, Esrefoglu M, et al. Protective effect of beta-glucan on acute lung injury induced by lipopolysaccharide in rats. *Turk J Med Sci* 2015; 45: 261–267.
3. Chen HI, Kao SJ, Wang D, et al. Acute respiratory distress syndrome. *J Biomed Sci* 2003; 10: 588–592.
4. Cross CE, Forte T, Stocker R, et al. Oxidative stress and abnormal cholesterol metabolism in patients with adult respiratory distress syndrome. *J Lab Clin Med* 1990; 115: 396–404.
5. Sabarirajan J, Vijayaraj P and Nachiappan V. Induction of acute respiratory distress syndrome in rats by lipopolysaccharide and its effect on oxidative stress and antioxidant status in lung. *Indian J Biochem Biophys* 2010; 47: 278–284.
6. Domenici-Lombardo L, Adembri C, Consalvo M, et al. Evolution of endotoxin induced acute lung injury in the rat. *Int J Exp Pathol* 1995; 76: 381–390.
7. Grommes J and Soehnlein O. Contribution of neutrophils to acute lung injury. *Mol Med* 2011; 17: 293–307.
8. Moraes TJ, Zurawska JH and Downey GP. Neutrophil granule contents in the pathogenesis of lung injury. *Curr Opin Hematol* 2006; 13: 21–27.
9. Al-Harbi NO, Imam F, Nadeem A, et al. Riboflavin attenuates lipopolysaccharide-induced lung injury in rats. *Toxicol Mech Methods* 2015; 25: 417–423.
10. Akramiene D, Kondrotas A, Didziapetriene J, et al. Effects of beta-glucans on the immune system. *Medicina (Kaunas)* 2007; 43: 597–606.
11. Fisher BJ, Seropian IM, Kraskauskas D, et al. Ascorbic acid attenuates lipopolysaccharide-induced acute lung injury. *Crit Care Med* 2011; 39: 1454–1460.
12. Matuschak GM and Lechner AJ. Acute lung injury and the acute respiratory distress syndrome: pathophysiology and treatment. *Mo Med* 2010; 107: 252–258.
13. Dickey BF, Thrall RS, McCormick JR, et al. Oleic-acid-induced lung injury in the rat. *Am J Pathol* 1981; 103: 376–383.
14. Zaeemzadeh N, Hemmati A, Arzi A, et al. Protective effect of caffeic acid phenethyl ester (CAPE) on amiodarone-induced pulmonary fibrosis in rat. *Iran J Pharm Res* 2011; 10: 321–328.
15. Blackwell TS, Blackwell TR, Holden EP, et al. In vivo anti-oxidant treatment suppresses nuclear factor-kappa B activation and neutrophilic lung inflammation. *J Immunol* 1996; 157: 1630–1637.
16. Covarrubias-Pinto A, Acuna AI, Beltran FA, et al. Old things new view: ascorbic acid protects the brain in neurodegenerative disorders. *Int J Mol Sci* 2015; 16: 28194–28217.

17. Du J, Cullen JJ and Buettner GR. Ascorbic acid: chemistry, biology and the treatment of cancer. *Biochim Biophys Acta* 2012; 1826: 443–457.

18. Wilson JX. Mechanism of action of vitamin C in sepsis: ascorbate modulates redox signaling in endothelium. *Biofactors* 2009; 35: 5–13.

19. Premkumar K and Bowlus CL. Ascorbic acid does not increase the oxidative stress induced by dietary iron in C3H mice. *J Nutr* 2004; 134: 435–438.

20. Halliwell B. Vitamin C: antioxidant or pro-oxidant in vivo? *Free Radic Res* 1996; 25: 439–454.

21. Neuzil J, Thomas SR and Stocker R. Requirement for, promotion, or inhibition by alpha-tocopherol of radical-induced initiation of plasma lipoprotein lipid peroxidation. *Free Radic Biol Med* 1997; 22: 57–71.

22. Borrelli E, Roux-Lombard P, Grau GE, et al. Plasma concentrations of cytokines, their soluble receptors, and antioxidant vitamins can predict the development of multiple organ failure in patients at risk. *Crit Care Med* 1996; 24: 392–397.

23. Brown LA, Harris FL and Jones DP. Ascorbate deficiency and oxidative stress in the alveolar type II cell. *Am J Physiol* 1997; 273: L782–L788.

24. Deng W, Deng Y, Deng J, et al. Losartan attenuated lipopolysaccharide-induced lung injury by suppression of lectin-like oxidized low-density lipoprotein receptor-1. *Int J Clin Exp Pathol* 2015; 8: 15670–15676.

25. Mu E, Ding R, An X, et al. Heparin attenuates lipopolysaccharide-induced acute lung injury by inhibiting nitric oxide synthase and TGF-beta/Smad signaling pathway. *Thromb Res* 2012; 129: 479–485.

26. Rydell-Tormanen K, Andreasson K, Hesselstrand R, et al. Extracellular matrix alterations and acute inflammation: developing in parallel during early induction of pulmonary fibrosis. *Lab Invest* 2012; 92: 917–925.

27. Noworyta-Sokolowska K, Gorska A and Golembiowska K. LPS-induced oxidative stress and inflammatory reaction in the rat striatum. *Pharmacol Rep* 2013; 65: 863–869.

28. Ho HL, Huo TI, Chang T, et al. Ascorbate lacks significant influence in rats with bile duct ligation-induced liver injury. *J Chin Med Assoc* 2017; 80: 539–550.

29. John DB and Gamble M. *Theory and practice of histological techniques.* 5th ed. Edinburgh: Elsevier, 2001.

30. Vyalov SL, Gabbiani G and Kapanci Y. Rat alveolar myofibroblasts acquire alpha-smooth muscle actin expression during bleomycin-induced pulmonary fibrosis. *Am J Pathol* 1993; 143: 1754–1765.

31. Glauert AM and Lewis P. *Biological specimen preparation for transmission electron microscopy.* 1st ed. London: Portland Press, 1998.

32. Kenyon NJ, Ward RW, McGrew G, et al. TGF-beta1 causes airway fibrosis and increased collagen I and III mRNA in mice. *Thorax* 2003; 58: 772–777.

33. Kranenburg AR, Willems-Widyastuti A, Moori WJ, et al. Enhanced bronchial expression of extracellular matrix proteins in chronic obstructive pulmonary disease. *Am J Clin Pathol* 2006; 126: 725–735.

34. Xing J and Birukova AA. ANP attenuates inflammatory signaling and Rho pathway of lung endothelial permeability induced by LPS and TNFalpha. *Microvasc Res* 2010; 79: 56–62.

35. Birukova AA, Tian X, Cokic I, et al. Endothelial barrier disruption and recovery is controlled by substrate stiffness. *Microvasc Res* 2013; 87: 50–57.

36. Moore B, Lawson WE, Oury TD, et al. Animal models of fibrotic lung disease. *Am J Respir Cell Mol Biol* 2013; 49: 167–179.

37. Zhuan-Yun LI, Xue-Ping Y, Bin L, et al. Auricularia auricular-judae polysaccharide attenuates lipopolysaccharide-induced acute lung injury by inhibiting oxidative stress and inflammation. *Biomed Rep* 2015; 3: 478–482.

38. Kim HJ, Jeong JS, Kim SR, et al. Inhibition of endoplasmic reticulum stress alleviates lipopolysaccharide-induced lung inflammation through modulation of NF-kappaB/HIF-1alpha signaling pathway. *Sci Rep* 2013; 3: 1142.

39. Parra ER, Pincelli MS, Teodoro WR, et al. Modeling pulmonary fibrosis by abnormal expression of telomerase/apoptosis/collagen V in experimental usual interstitial pneumonia. *Braz J Med Biol Res* 2014; 47: 567–575.

40. Tamiolakis D, Papadopoulos N, Hatzimichael A, et al. A quantitative study of collagen production by human smooth muscle cells during intestinal morphogenesis. *Clin Exp Obstet Gynecol* 2002; 29: 135–139.

41. Segnani C, Ippolito C, Antonioli L, et al. Histochemical detection of collagen fibers by Sirius Red/Fast Green is more sensitive than van Gieson or Sirius Red alone in normal and inflamed rat colon. *PLoS One* 2015; 10: e0144630.

42. Whittaker P, Kloner RA, Boughner DR, et al. Quantitative assessment of myocardial collagen with picrosirius red staining and circularly polarized light. *Basic Res Cardiol* 1994; 89: 397–410.

43. Junqueira LC, Bignolas G and Brentani RR. Picrosirius staining plus polarization microscopy, a specific method for collagen detection in tissue sections. *Histochem J* 1979; 11: 447–455.

44. Zhang K and Phan SH. Cytokines and pulmonary fibrosis. *Biol Signals* 1996; 5: 232–239.

45. Day BJ. Antioxidants as potential therapeutics for lung fibrosis. *Antioxid Redox Signal* 2008; 10: 355–370.

46. Cross CE and Eiserich JP. Oxidative stress in acute lung injury: Deja vu or something new? *Crit Care Med* 2004; 32: 892–893.

47. Naidu KA. Vitamin C in human health and disease is still a mystery? An overview. *Nutr J* 2003; 2: 7.

48. King TE Jr, Albera C, Bradford WZ, et al. Effect of interferon gamma-1b on survival in patients with idiopathic pulmonary fibrosis (INSPIRE): a multicentre, randomised, placebo-controlled trial. *Lancet* 2009; 374: 222–228.

49. Adler KB, Callahan LM and Evans JN. Cellular alterations in the alveolar wall in bleomycin-induced pulmonary fibrosis in rats. *Am Rev Respir Dis* 1986; 133: 1043–1048.

50. Evans JN, Kelley J, Low RB, et al. Increased contractility of isolated lung parenchyma in an animal model of pulmonary fibrosis induced by bleomycin. *Am Rev Respir Dis* 1982; 125: 89–94.

51. Levental KR, Yu H, Kass L, et al. Matrix crosslinking forces tumor progression by enhancing integrin signaling. *Cell* 2009; 139: 891–906.

52. Dawson W and West GB. The nature of the antagonism of bronchospasm in the guinea-pig by ascorbic acid. *J Pharm Pharmacol* 1965; 17: 595–596.

53. Raghu G, Brown KK, Costabel U, et al. Treatment of idiopathic pulmonary fibrosis with etanercept: an exploratory, placebo-controlled trial. *Am J Respir Crit Care Med* 2008; 178: 948–955.